ELECTRONICS AND ELECTRICAL ENGINEERING
ISSN 1392 – 1215 *2010. No. 4(100)*
ELEKTRONIKA IR ELEKTROTECHNIKA

ELECTRONICS
T 170
ELEKTRONIKA

The Investigation of Magnetic Field Distribution in a Railway Rail Area

A. Dumčius
Department of Electronics Engineering, Kaunas University of Technology,
Studentų str. 50-142, LT-51368 Kaunas, Lithuania, phone: +370 37 300520, e–mail: antanas.dumcius@ktu.lt
V. Augutis, D. Gailius
Department of Electronic and Measurement Systems, Kaunas University of Technology,
Studentų str. 50-445, LT-51368 Kaunas, Lithuania, phone: +370 37 451617, e–mails: vygantas.augutis@ktu.lt; darius.gailius@ktu.lt

Introduction

Railway traffic safety systems consists of the three main subsystems: information signal formation equipment, signal transmission lines and signal information reception and processing devices. Carrier pulse-pause modulation or frequency modulation is typically used in such systems to encode the information. Assume that the information in the system is encoded using the durations of pulses and pauses. During the signal transmission the signaling modulated currents with frequencies of 25 Hz, 50 Hz or 75 Hz flow over the line (railway rails). The amplitudes of these currents may vary from 1.4 A to 25 A in respect of the receiver location. Currents with frequencies of 50 Hz also flow over the electric traction railway lines and the amplitudes of these currents may reach 500-600 A.

Currents flowing over the railway rails create the alternating magnetic fields. In one of them the information for the safety system is encoded, and in the other which is created by the traction current the potential disturbances for the safety system are present. Besides these fields, the magnetic fields may be present in the railway rail area which are induced due to the magnetization of the rails and the adjacent ferromagnetic constructions. Furthermore the Earth's magnetic field is also active in the railway rail area.

Railway rails magnetization arises because of the several reasons: 1. During the technological process of rail manufacture. Magnetization is uneven along the rail and the magnetic field strength at the ends of the rail reaches 6000-10000 A/m, and the all causes of magnetization are not clear [1]. 2. During the electro welding by melting of the rail into the junction-less sections, the current of 45-50 kA flows over the rail during the welding [2]. This current induces the magnetic field distributed around the rail and inside of it. The welding process is rapid, the metal is melted only in a thin layer and at the temperature at the adjacent layers is lower than the Curie point temperature of the railway-grade steel (768° C) [3]. The railway rail welding process supposedly ends when the temperature reaches 370^0 C [3]. Therefore the residual magnetization may be present at the welding point of the cooled rail. 3. During the exploitation of the rails the magnetization changes under the cyclic loads due to the magnetoelastic effect [4]. In most cases the magnetic field induced by the traction currents and the magnetization of the rails are the main sources of the safety system disturbances. During the train ride the encoded information signals are induced in the information signal reception coils which are mounted at the front of the locomotive; and when the rail magnetization is present, the interfering signals are also induced and their amplitude is related to the magnetic field vector and the movement velocity.

Mathematical models

In order to research the magnetic field distribution in the railway rail area it is purposeful to apply the computer-based modeling [5–7].

The magnetic field is generated by the signal and traction currents. In this case we are interested not in the transient processes but in the maximum amplitudes of the magnetic fields, therefore only the static case will be considered, suppose at the time of signal current maximum. Model is built for the R65 type rail the cross-section area of which is 82.65 $cm^{2.}$ The configuration of the rail cross-section is substituted for the circle of the equivalent area with the diameter of 10.26 cm. The model is created for the 2D geometry; the current is evenly distributed over the area and flows perpendicularly the cross-section in opposite directions in both rails of the line. The coils with the core the magnetic permeability of which is $\mu_c = 10$ are fastened 150 mm above the upper surface of the rail.

For the case of magneto static and quasi-static fields, Ampere's law can by written as

$$\sigma\frac{\delta\mathbf{A}}{\delta t}+\nabla(\frac{\nabla\mathbf{A}}{\mu_0}-\mathbf{M})-\sigma\mathbf{v}\nabla\mathbf{A}+\sigma\nabla\mathbf{V}=\mathbf{J}^e, \quad (1)$$

where **A** – the magnetic vector potential; **M** – the magnetization vector; **v** – the velocity of conductors; **V** – the electric potential vector; $\mathbf{J}^e$ – the externally applied current density.

In this case it is necessary to calculate the maximum values of the intensity of magnetic field created by signal current flowing in the rails.

Assuming that conductors, field and current are static, the magnetic vector potential **A** must satisfy the following equation

$$\nabla(\frac{\nabla\mathbf{A}}{\mu_0})=\mathbf{J}^e. \quad (2)$$

The relation between magnetic flux density **B** and magnetic vector potential **A** and magnetic field density is given by

$$\mathbf{B}=\nabla\cdot\mathbf{A}, \quad (3)$$

$$\mathbf{B}=\mu_0\mu\,\mathbf{H}. \quad (4)$$

The parameters of magnetic field it is calculated in the zone from the surface of conductor to the fixed point in which it is possible to consider that the intensity of magnetic field is close to zero.

The boundary condition for the exterior boundary, that is, the circle external surface, where conditions corresponding to zero magnetic flux

$$\mathbf{n}\cdot\mathbf{A}=0, \quad (5)$$

where **n** is the outward normal from circle external surface, and for interior boundaries, that is, the conductors external surface, were conditions assume continuity, corresponding to a homogenous Neumann condition

$$\mathbf{n}\,(\mathbf{H}_1-\mathbf{H}_2)=0, \quad (6)$$

where **n** is the outward normal from external surface of conductors, $\mathbf{H_1}$ and $\mathbf{H_2}$ is the intensity of magnetic field on the external and internal surface of conductors respectively.

The model for calculation on magnetic field of signal current was built using the 2D Perpendicular Induction Currents, Vector Potential application mode. The modeling plane is a cross section of the two rail, two receiving coils with the cores and the surrounding air. The applied current in the conductors was in rage from 1.4 A to 25 A, but with different signs.

The model for calculation on magnetic field of rail welding current was built similarly by using the 2D Perpendicular Induction Currents, Vector Potential application mode. The applied current in the rail was 50kA.

In the simulation was used the finite elements method and the program COMSOL Multiphysics.

During the simulation the magnetic field change was investigated by varying the strength of the signal current within the range of the real fluctuation (from 1.4 A to 25 A) and by increasing the distance from the rail surface to the centre of the core of the receiving coil (200 mm). The magnetic field components and the flux density were calculated while changing the magnetic permeability of the core from 5 to 100.

Results of magnetic field simulation

For illustrative purposes the magnetic field flux distribution in the railway rail area when the current of 1.4 A flows over the rail is given in the Fig. 1.

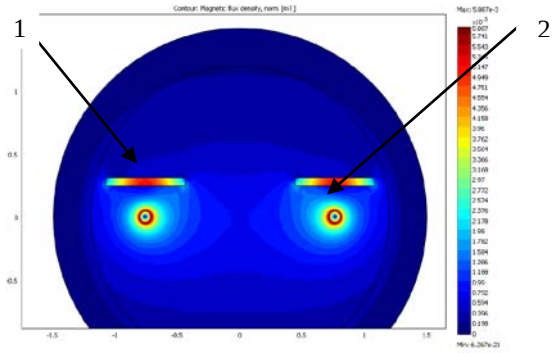

Fig. 1. Magnetic flux density in the rail area, mT, where 1 – receiving coil's core; 2 – conductor whose cross-section is equivalent to the rail cross-section

The distribution of the magnetic field component Hx induced by the signal current (25 A) in the air gap between the top of the rail and the core of the receiving coil is shown in Fig. 2, and for the component Hy – in Fig. 4.

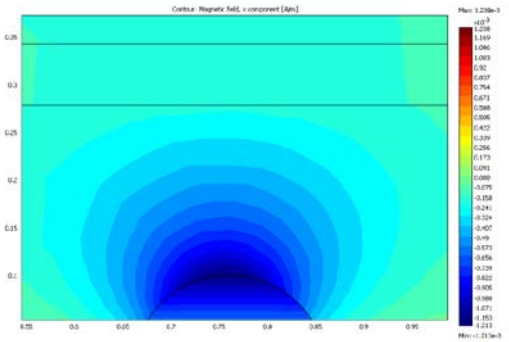

Fig. 2. Distribution of the magnetic field component Hx: I = 25 A; $H_{x\,max}$ = 128.9 A/m near conductor surface, $H_{x\,min}$ = 0.49 A/m within receiving coil core

The distribution of the strength of the magnetic field component Hx in respect of the distance from the top of the rail for the marginal magnitudes of the signal current (1.4 A and 25 A) according to the simulation results is given in Fig. 3.

The dependency of the magnetic flux inside the core of the coil on the magnetic permeability of the core is presented in Fig. 5.

The flux varies less when the permeability μ_c is higher than 50. The magnetic permeability of the coil core was determined experimentally (the receiving coil operated for five years was analyzed by measuring the coil inductance with core and without it) and it was μ_c = 8.66.

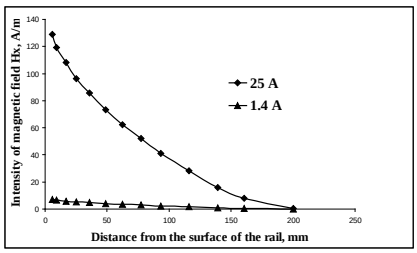

Fig. 3. The change of the magnetic field component Hx when increasing the distance from the surface of the rail, under the signal currents of 1.4 A and 25 A

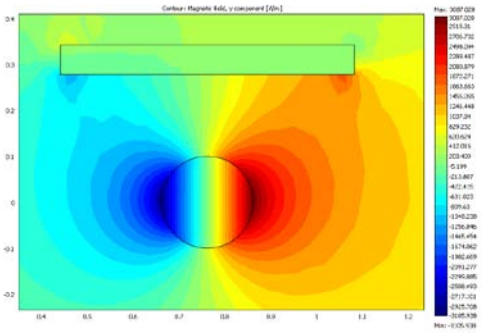

Fig. 4. The distribution of the magnetic field component Hy: I= 25 A; Hy_{max} = 149.36 A/m near conductor surface, $H_{y\ min}$ = 0.0169 A/m within receiving coil core

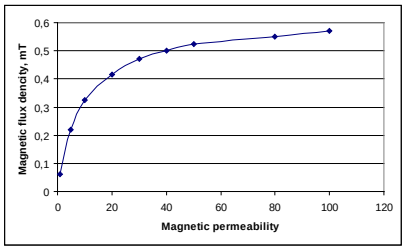

Fig. 5. The dependence of the magnetic flux in the core of the coil on the magnetic permeability of the core μ_c

Thus the changes in the magnetic permeability of the core during the exploitation may significantly influence the amplitude of the received signal.

The simulation results of the magnetic field induced by the welding current during the process of the welding are shown in Figs. 6–8.

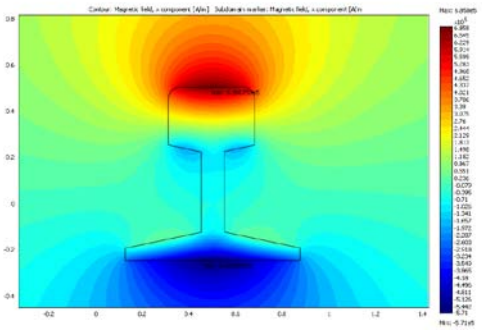

Fig. 6. The distribution of the magnetic field component Hx at the surface of the rail, Hx = $6.6 \cdot 10^5$ A/m

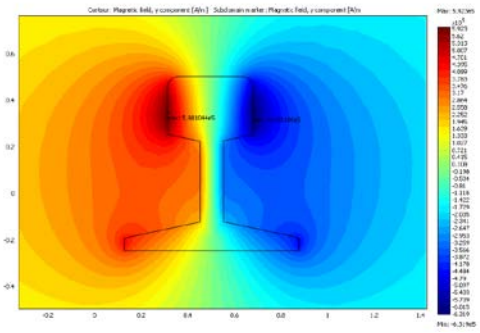

Fig. 7. The distribution of the magnetic field component Hy

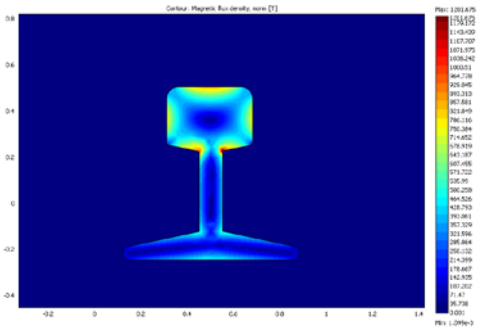

Fig. 8. The districution of the magnetic flux within the cross-section of the rail

Results of measurements

The measurements of the rail magnetization were performed at the different points of the railroad lines and at the rail welding plant using the developed magnetic field measurement device Some of the measurement results for illustrative purposes are given in Figs. 9–12.

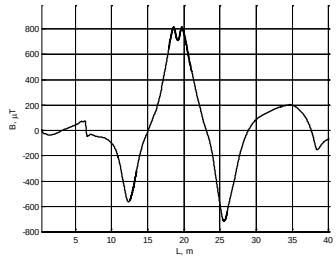

Fig. 9. The distribution of the vertical component of the magnetic flux density induced by rail magnetization, measured along the rail

In order to evaluate the influence of the welding the rail magnetizations before and after the welding (into continuous section) were measured. To illustrate this the distribution of the vertical component of the magnetic flux density at the two ends of the rail (A and B, the prospective welding seam) is shown in Fig. 9 and Fig. 10.

The measurements of the welded rails (Fig. 11) indicate that the distribution of the magnetic flux density at the area of the welding seam according to its nature is similar to the former distribution at the ends of the rails prepared for the welding.

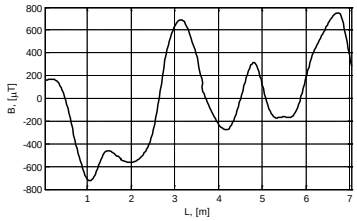

Fig. 10. The distribution of the magnetic flux density in the rail A before the welding

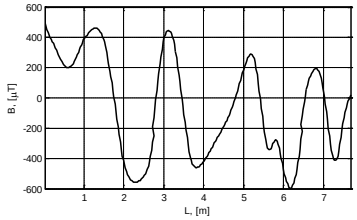

Fig. 11. The distribution of the magnetic flux density in the rail B before the welding

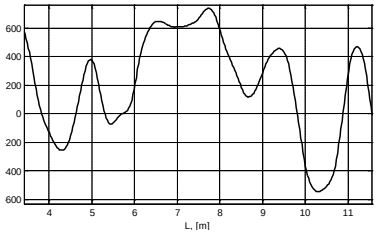

Fig. 12. The distribution of the magnetic flux density at the area of the welding seam after the welding of the rails A and B

Conclusions

1. The magnetic flux density at some magnetization areas of railroad rails can be of order or more higher than the generated minimal signal currents, consequently during the locomotive ride it can induce the interferences in its traffic safety system conditioning the emergency breaking of the locomotive.
2. During the measurements of new rails the magnetization areas spaced with some certain periodicity were determined, additionally there are magnetizations at the ends of the rails.
3. During the rail electro welding by melting a strong magnetic field is induced in the rail and its area. It can influence the orientation of magnetic domains in the areas of the welding seam in which the temperature is lower than the Curie point.
4. It was determined that after the rail electro welding by melting the distribution of the magnetic flux density at the area of the welding seam changed insignificantly.
5. Due to the uneven distribution of the magnetic flux inside of the rail during the welding the surface of rail head should be magnetized more intensely.
6. During the simulation the relation between the amplitude value of the signal in the reception coils of the locomotive safety system and the coil distance from the rail and its mounting location in respect of the center of the realhead was determined.
7. More detailed research is required to determine the causes of the rail magnetization.

References

1. **Антонов А. С., Козлов А. А., Козлов А. С., Семенов В. Т., Ушаков А. Е.** Намагниченность релсов // Путь и путевое хозяйство. 2008. – №. 2(14). – С. 6–7.
2. Welding Rail. http://southern.railfan.net/ties/1966/66-9/weld.html
3. Сварка рельсов в пути на железных дорогах Северной Америки. http://www.css-rzd.ru/zdm/02-2003/02033.htm
4. **Antipov G. A., Korolev M. Yu.** Magnetic Viscosity of Rail Steel and its Influence on Magnetization of Rails Tested by High-Rate Magnetic Flaw Detection Methods // Russian Journal of Nondestructive Testing. 2002. – Vol. 38, no. 6. P. 438–446.
5. **Boudiaf A.** Numerical Magnetic Field Computation in a Unilateral Linear Asynchronous Motor without Inverse Magnetic Circuit // Electronics and Electrical Engineering. – Kaunas: Technologija, 2007. – No. 2(90). – P. 81–84.
6. **Bartkevičius S., Novickij J.** The Investigation of Magnetic Field Distribution of Dual Coil Pulsed Magnet // Electronics and Electrical Engineering. – Kaunas: Technologija, 2009. – No. 4(92). – P. 23–26.
7. Calculation Program of Effective Impedances, Magnetic and Electric Field Distribution of Catenary Lines. http://www.elbas.ch/pdf/ELBASTOOL_4_EN.pdf

Received 2010 01 25

A. Dumčius, V. Augutis, D. Gailius. The Investigation of Magnetic Field Distribution in a Railway Rail Area // Electronics and Electrical Engineering. – Kaunas: Technologija, 2010. – No. 4(100). – P. 95–98.

The distribution of the magnetization of the rails of railroad line is examined. The specific distribution of the magnetization exceeding the permitted level can cause errors in the traffic safety system during the motion of locomotive, leading to the automatic braking of locomotive. The results of simulation and measurements are given. Ill. 12, bibl. 7 (In English; summaries in English, Russian and Lithuanian).

А. Думчюс, В. Аугутис, Д. Гайлюс. Исследование намагниченности желездорожного рельса // Электроника и электротехника. – Каунас: Технология, 2010. – №. 4(100). – С. 95–98.

Рассматривается распределение намагниченности рельсов железнодорожной линии. Определенное распределение намагниченности, превышающей допустимы уровень, при движении локомотива может вызвать сбои в системе обеспечения безопасности движения, приводящие к автоматическому торможению локомотива. Приведены результаты моделирования и измереный. Ил. 12, библ. 7 (на английском языке; рефераты на английском, русском и литовском яз.).

A. Dumčius, V. Augutis, D. Gailius. Magnetinio lauko pasiskirstymo geležinkelio bėgyje tyrimas // Elektronika ir elektrotechnika. – Kaunas: Technologija, 2010. – Nr. 4(100). – P. 95–98.

Nagrinėjamas magnetinio lauko pasiskirstymas geležinkelio bėgyje. Esant tam tikram bėgių įmagnetinimo pasiskirstymui, kai lauko stipris viršija tam tikrą ribą, važiuojančio lokomotyvo jo eismo saugos sistemoje gali atsirasti trikdžių, dėl kurių automatiškai stabdomas lokomotyvas. Pateikti modeliavimo ir matavimų rezultatai. Il. 12, bibl. 7 (anglų kalba; santraukos anglų, rusų ir lietuvių k.).